First-principles simulations of structural, electronic, and magnetic properties of vacancy-bearing Fe silicates

Swastika Chatterjee and Tanusri Saha-Dasgupta*
Department of Material Sciences, S. N. Bose National Center for Basic Sciences, JD-Block, Sector-III, Salt Lake City, Kolkata 700 098, India

(Received 27 October 2009; revised manuscript received 2 March 2010; published 7 April 2010)

We study the structural, electronic, and magnetic properties of vacancy-bearing silicate mineral, Fe_2SiO_4 using first-principles density-functional theory (DFT). Our DFT-simulated structure, which is compositionally close to naturally occurring laihunite compound shows good agreement in the general trend in the change in Fe_2SiO_4 crystal structure upon vacancy introduction. Our study shows that the introduction of vacancy creates charge disproportionation of Fe ions into Fe^{2+}-like and Fe^{3+}-like ions with a charge difference larger than 0.5, keeping the valences of other ions unaltered. Fe^{2+}-like ions are found to occupy octahedral sites of specific symmetry while Fe^{3+}-like occupy the other leading to charge ordering at zero temperature. We also study the magnetic ordering of Fe ions.

DOI: 10.1103/PhysRevB.81.155105 PACS number(s): 71.20.Be, 91.32.Gh

I. INTRODUCTION

Application of first-principles calculations to the study of properties of complex earth forming minerals has emerged in recent years as a powerful addition[1–5] to experimental studies in mineral physics. The minerals containing 3*d* transition metal ions such as Fe pose challenges[6] in this respect due to the interplay of charge, spin, and orbital, and the strong electron-electron correlation effect at the Fe site. Proper description of such minerals and their properties therefore requires application of developed techniques that can handle the correct material specific aspects as well as the effects caused by the strong electron-electron correlation. The successful description of these complex minerals, in turn, establishes the reliability of the first-principles techniques on dealing the complexity of mineral physics, thereby expanding the scope of application of the ideas developed in condensed matter physics to systems and processes of geophysical interest. In the following, we put a step forward in establishing this philosophy by considering the example of vacancy-bearing fayalite (Ref. 7) (Fe_2SiO_4), end member of $(Mg,Fe)_2SiO_4$ olivines, one of the most abundant minerals in Earth's upper mantle.

The octahedral sites in olivine, in general, can be occupied by divalent cations M^{2+} (e.g., Fe^{2+}, Mg^{2+}, Co^{2+}, and Mn^{2+}). Large number of studies have addressed site occupancies and ordering of divalent octahedral cation in olivines.[8–11] Very recently the site preference problem in Mg-Fe olivine has been also studied using first-principles density-functional calculations.[12] In contrast, less number of studies have been carried out for minerals bearing significant quantities of trivalent cations at the octahedral sites. Laihunite,[13–15] an intermediate temperature oxidation product of fayalite[16] is the best known example of such mineral. Published literature on laihunite compounds are of varying composition but follow the general formula[17] $\square_x Fe_{2-x}SiO_4$ where $\square$ represents vacancies and x can range from 0.24 to 0.5. There do exist a few experimental studies on laihunite: e.g., Mössbauer spectroscopy study was carried by Kan and Coey[18] to investigate the magnetic and electrical properties of laihunite, as well as studies have been devoted to structural determination of laihunite through x-ray spectroscopy[13,19,20] and high-resolution transmission electron microscopy.[17] The theoretical studies, on the other hand, in understanding this defect structure are minimal. In particular, there has been no report of the first-principles calculations of this class of mineral, which provides the interesting situation of mixed valency of Fe ions, leading to possibility of charge disproportionation and charge ordering at Fe site that has drawn the attention of physicists since years considering the example of magnetite (Fe_3O_4) (Ref. 21) and manganites [e.g., $La_{0.5}Ca_{0.5}MnO_3$ (Ref. 22)]. In this paper, we present a detailed study of the structural, electronic, and magnetic properties of laihunite with $x=0.5$. For this purpose we start with a pure fayalite mineral with formula Fe_2SiO_4, in which we introduce vacancies to arrive at a compound with chemical formula $\square_{0.5}Fe_{1.5}SiO_4$. The site preference of vacancy formation is determined through first-principles DFT calculations. Strong electron-electron correlation effect and the magnetism at Fe site in high spin state is achieved through the local spin-density approximation (LSDA)+U calculations. The crystal structure of the vacancy introduced fayalite is then optimized to generate the crystal structure of the laihunite. The DFT optimized structure show good agreement in qualitative trend with available crystal-structure data of laihunite though with somewhat different chemical composition[13] of $\square_{0.4}Fe_{1.6}SiO_4$. The study of the calculated electronic structure shows that the introduction of the vacancy drives the Fe ion into the mixed valent state of $Fe^{2.67+}$, keeping the valences of the other components intact. The mixed valent Fe ions subsequently charge disproportionate to Fe^{2+}-like and Fe^{3+}-like ions, with Fe^{3+}-like ions preferentially occupying the octahedra with a particular site symmetry and Fe^{2+}-like ions occupying the octahedra with another site symmetry. This preferential occupation originates due to the particular structural distortion that results upon introduction of the vacancy. The preferential occupancy of Fe^{3+}-like ions to one particular type of octahedral site and Fe^{2+}-like ions to another causes the charge ordering at zero temperature. We also study the underlying magnetic ordering.

The paper is organized as follows. Section II describes the methodology and the computational details. This is followed up by results in Sec. III, which is divided into several subsections. Section III A describes the study of the site preference of vacancy formation while Sec. III B describes the optimized crystal structure of laihunite, which is formed upon introduction of vacancies into fayalite. Section III C describes the electronic and magnetic structure of laihunite as calculated within the framework of DFT. The paper concludes with discussion and summary in Sec. IV.

II. METHODOLOGY AND COMPUTATIONAL DETAILS

We have used parameter-free density-functional theory (DFT) (Ref. 23) for our study. We considered a combination of two different methods, namely: a plane wave-based method as implemented in the Vienna *ab initio* simulation package (VASP) (Ref. 24) and the muffin-tin-orbital- (MTO-) based linear muffin-tin orbital method[25] as implemented in Stuttgart TBLMTO-47 code. The accuracy of calculations within the basis set of the two methods has been checked with respect to each other. For plane-wave calculations we have used projector augmented wave potentials[26] and the wave functions were expanded in the plane-wave basis with a kinetic-energy cutoff of 500 eV. Reciprocal space integration was carried out with a k mesh of $6\times6\times6$. For our LMTO calculations, we have used six different empty spheres for fayalite and twenty different empty spheres for vacancy-bearing fayalite to achieve the space filling, and considered the valence configuration of Fe $3d4s4p$, Mg $3s3p$, Si $3s3p$, and O $2s2p$.

In order to take into account the missing correlation effect beyond the local spin-density approximation, which turns out to be important for the proper description of Fe-derived states we have carried out LSDA+U (Ref. 27) calculations, where U is the on-site Coulomb repulsion within the self-interaction correction for the double counting.[28] We have also performed calculations with around mean field scheme in order to check the influence of different implementations of double-counting correction, if any. The results were found to be qualitatively same. For all the calculations performed we have fixed the value of U at a typical[29] value of 4.5 eV while the Hund's exchange J introduced to consider the multiorbital situation, is chosen to be 0.8 eV.

In this present work since we study the role of vacancy in silicate mineral, structural relaxation plays an important role as once a vacant site is created the neighboring atoms are expected to relax. For fayalite with no vacancy we have carried out relaxation of the atomic positions keeping the lattice constants fixed at the experimentally estimated values. This was done due to the fact that the x-ray diffraction studies may not accurately determine the position of light atoms such as oxygen. Moreover, the experimental data are from actual minerals that may have been formed under diverse conditions. In the case of structures with vacancy, the positions of the vacant atomic sites were selected judiciously and a complete relaxation was performed where the shape and volume of the cell were allowed to relax in addition to atomic positions. The conjugate gradient algorithm was used for the relaxation calculations. All relaxations were performed using plane wave pseudopotential method employing the VASP code.

TABLE I. Energy required for creation of vacancy at different atomic sites of fayalite.

Site	Energy (eV)	Site	Energy (eV)
M1	6.65	O1	9.99
M2	9.17	O2	9.80
Si	10.92	O3	9.86

III. RESULTS

A. Site preference of vacancy

The formation energy of a single vacancy, i.e, the energy associated with removing a single ion from the lattice to an isolated state, calculated using LSDA+U total energies with plane-wave basis are tabulated in Table I for vacancies created on different sites of pure fayalite.

Fayalite, an olivine structured mineral can be viewed as a distorted hexagonal close packed (HCP) array of oxygen ions [shown in Fig. 1(A)], with half of the octahedral sites and one-eighth of the tetrahedral sites occupied by Fe and Si, respectively. There are two symmetry distinct octahedral

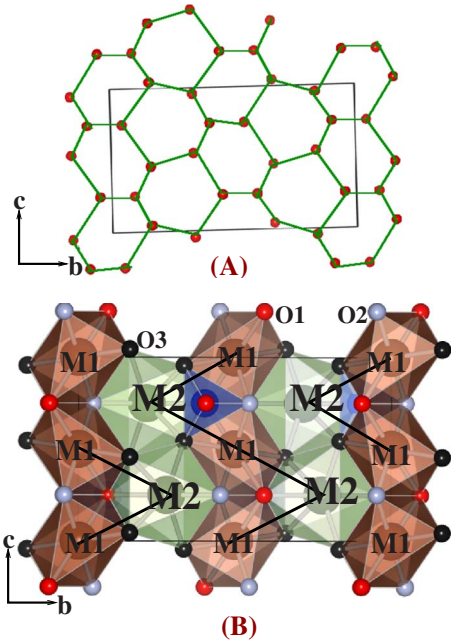

FIG. 1. (Color online) (A) Schematic showing the approximate hexagonal closed packing of oxygen atoms in case of fayalite projected on to the *bc* plane. (B) The total structure of fayalite. Large, medium, and small atoms designate Fe, Si, and O atoms. The red (dark) octahedra are the $M1O_6$ octahedra and green (light) octahedra are $M2O_6$ octahedra. The three distinct oxygen atoms O1, O2, and O3 have been marked. The solid line depicts the zigzag chain connecting the nearest-neighboring M1 and M2 octahedra.

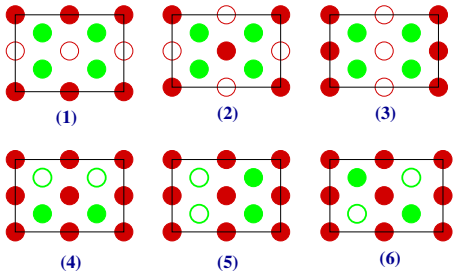

FIG. 2. (Color online) Schematic showing different configurations with all possible ways in which two vacancies can be created at the metallic sites in fayalite. The Si and O degrees of freedom have been omitted out from the figure for clarity. Red (dark) and green (light) filled circles represent M1 and M2 sites, respectively. The empty circles depict the vacant octahedral site.

sites: M1, on a center of symmetry and M2, on a mirror plane. There is only one distinct tetrahedral site, and three distinct oxygen sites, O1 and O2 on the mirror plane and O3 in a general position [see Fig. 1(B)]. The nearest-neighbor M1 and M2 sites form a zigzag chain running in *bc* plane. As it is clearly seen from Table I, M1 site is the most preferred site for vacancy creation, followed by M2 site, while the hardest site to create vacancy is Si. Among the oxygen sites, O2 is found to be more favorable compared to O3 and O1. The formation energies quoted in Table I, were obtained by considering single vacancy in one unit cell of fayalite. We have checked the reliability of our result by considering a supercell of $2\times2\times2$, the general trend is found to be the same. The computational effort prohibits us to go to larger supercells. In principle, to get an accurate estimate of vacancy formation energy, one should carry out calculations with increasing dimension of the cell and check the convergence of the defect energy. Since we are interested in finding out the general trend in terms of the most favorable position for vacancy formation rather than an accurate estimate of vacancy-formation energy, the calculated numbers using one unit cell serve our purpose. The previous calculations[30] for Forsterite (Mg_2SiO_4) using atomistic method of modeling with interatomic potentials which carefully checked the convergence with increasing cell size also find M1 to be the most favorable position for vacancies.

B. Crystal structure of laihunite

In order to create laihunite with a formula $\square_{0.5}Fe_{1.5}SiO_4$ out of fayalite, one needs to introduce two vacancies in a unit cell of fayalite which contains 4 f.u. Following our analysis presented in previous section, we choose M1 and M2 sites for creation of this double vacancies. There are in total four M1 sites and four M2 sites in a unit cell and double vacancies at M1 and M2 site can be created in six distinct ways. The distinct configurations are shown in Fig. 2 and the total energies corresponding to the optimized geometries of these configurations are listed in Table II. As found, in case of single vacancy, the creation of double vacancies is also favored at M1 sites. Analysis of configurations with double vacancies at M1 sites, show configuration 1 to be of lowest energy, while the energy of the configuration where two vacancies sit in two neighboring M1 sites are significantly higher. This indicates that the vacancies disfavor cluster formation. Observation of such favorable configuration with M1 sites being occupied alternately by vacancy and Fe along the *c* axis has been suggested in experimental studies as well.[18]

TABLE II. Total energies corresponding to the six different configurations with double vacancies created at M1 and M2 sites in fayalite as shown in Fig. 2.

Configuration	Energy (eV)	Configuration	Energy (eV)
Configuration 1	−208.04	Configuration 4	−205.56
Configuration 2	−207.95	Configuration 5	−204.74
Configuration 3	−206.46	Configuration 6	−203.73

In the following, all the analyses are therefore carried out with configuration 1. The distortion of the HCP network of oxygen ions upon introduction of Fe^{2+} cations and Si ions at the octahedral and tetrahedral sites gives the fayalite crystal-structure orthorhombic symmetry with *Pbnm* space group. The introduction of vacancies in fayalite further reduces the symmetry. The optimized geometry in configuration 1 turned out to be that of triclinic. A comparison of the lattice constants between fayalite with and without vacancies show (see Table III) substantial contraction along *b* and *c* axes when vacancies are introduced, which as expected, leads to an overall reduction of the unit cell volume. While in fayalite there are six distinct classes of atoms, the lowering of symmetry in presence of vacancies gives rise to 14 different classes of atoms as listed in Table III. Splitting of M1 and M2 sites into inequivalent groups upon the reduction in symmetry for laihunite has been suggested in experiment.[18] Table IV lists all the free coordinates of the atomic positions. Figure 3 shows the geometry optimized structure of configuration 1 with distinct class of various atoms marked. In case of fayalite the $M2O_6$ octahedra centered about Fe2 ions are larger in volume and more distorted (measured in terms of root-mean-square deviation of the Fe-O bond length) compared to $M1O_6$ octahedra centered about Fe1 ion. The introduction of vacancies in case of $\square_{0.5}Fe_{1.5}SiO_4$ reverses this trend (see Table V), in the sense that the $M2O_6$ octahedra occupied by Fe3 and Fe4 become smaller in volume compared to $M1O_6$ occupied by Fe1 and Fe2. In Table V we also list these quantities corresponding to only available[13] crystal-structure data of laihunite of composition $\square_{0.4}Fe_{1.6}SiO_4$. We find that although the concentration of the vacancies are different between computed configuration 1 and experimentally measured crystal, the general trend in terms of comparison of bond lengths and distortions between $M1O_6$ and $M2O_6$ octahedra show good agreement with each other. The lattice constants (a=4.81 Å, b=10.19 Å, and c=5.80 Å) and volume [283.9 Å^3] of $\square_{0.4}Fe_{1.6}SiO_4$ also show good agreement with that of geometry optimized configuration 1 of $\square_{0.5}Fe_{1.5}SiO_4$ (a=4.77 Å, b=10.08 Å, c=5.73 Å, and volume=275.1 Å^3).

TABLE III. The lattice constants and Wykoff positions for each species for fayalite in orthorhombic *Pbnm* (crystallogrphic group no. 62) space group and configuration 1 in triclinic space group P-1 (crystallographic group no. 2).

	a (Å)	*b* (Å)	*c* (Å)	Atom	Class	Coordinates
Fayalite	4.82	10.47	6.07	Fe1	4*a*	(0,0,0), (1/2,1/2,0), (0,0,1/2), (1/2,1/2,1/2)
				Fe2, Si, O1, O2	4*c*	$(x,y,1/4)$, $(x+1/2,-y+1/2,3/4)$, $(-x,-y,3/4)$, $(-x+1/2,y+1/2,1/4)$
				O3	8*d*	(x,y,z), $(x+1/2,-y+1/2,-z)$, $(-x,-y,z+1/2)$, $(-x+1/2,y+1/2,-z+1/2)$, $(-x,-y,-z)$, $(-x+1/2,y+1/2,z)$, $(x,y,-z+1/2)$, $(x+1/2,-y+1/2,z+1/2)$
Configuration 1	4.77	10.08	5.73	Fe1	*a*	(0,0,0)
				Fe2	*e*	1/2,1/2,0
				Fe3, Fe4, Si1, Si2, O1 O2, O3, O4, O5, O6, O7, O8	2*i*	(x,y,z), $(-x,-y,-z)$

C. Electronic and magnetic structure of fayalite with double vacancies at the metallic sites

1. Basic electronic structure

In this section we describe the electronic structure of configuration 1 which is basically the fayalite structure with double vacancies at M1 sites. In fayalite each Fe atom sits at the center of the octahedron created by its six neighboring oxygen atoms. This octahedral field lifts the fivefold degeneracy of the Fe *d* states, splitting them it into two groups: the three lower t_{2g} levels and the two higher e_g levels.[31] This is schematically shown in Fig. 4. The difference in energy between these two levels is the crystal-field splitting energy, denoted as E_{CF}. There is a further splitting between the up- and down-spin channels due to exchange interaction denoted as E_{EX}. If E_{EX} is greater than E_{CF}, the up-spin channel will be occupied first followed by the down spin and the system is said to be in the high spin state. In case of fayalite Fe is found to be in the high spin state with a magnetic moment of $3.6\mu_B$.

Figure 5(A) presents the LSDA+*U* density of states for the vacancy bearing fayalite in configuration1 projected onto Fe *d*, O *p*, and Si *sp* states. The treatment of correlation effect within LSDA+*U* leads to insulating solution. This is supported by the activated conductivity observed in experiment.[18] The zero of the energy scale in Fig. 5(A) is set at the top of the valence band. It can be seen that there is negligible contribution from Si to the occupied part of the density of states (DOS). States close to the Fermi level are dominated basically by O *p* and Fe *d* where they strongly hybridize. The *d*-*p* hybridized band extends from −9.5 to 4 eV.

Figs. 5(B) and 5(C) show the Fe *d* density of states projected onto Fe1 and Fe2 atoms occupying M1 sites and Fe3 and Fe4 atoms occupying M2 sites, respectively. Focusing onto down spin channel, it is found to be nearly empty for Fe atoms occupying M2 sites while it is partially filled for atoms occupying M1 site. This gives rise to charge disproportionation between Fe ions occupying M1 (two in number) and M2 sites (four in number), with those occupying M1 sites being close to Fe^{2+} and those occupying M2 sites being close to Fe^{3+}. The charge difference between the two is found to be about 0.55. This leads us to conclude that the Fe ion in mixed valence state $Fe^{2.67+}$ in $\square_{0.5}Fe_{1.5}SiO_4$, charge disproportionates in following matter: 6 $Fe^{2.67+} \rightarrow 4$ Fe^{3+} +2 Fe^{2+}. The magnetic moments of Fe sites occupying M1 and M2 sites are found to be $3.7\mu_B$ and $4.3\mu_B$ respectively, supporting the charge disproportionation between M1 and M2 sites. The preferential occupancy of Fe^{2+}-like ions into

TABLE IV. Crystal structure data for configuration 1.

	Space group P-1	*a* 4.76656 (Å)	*b* 10.07953 (Å)	*c* 5.72763 (Å)	Alpha 88.5041	Beta 90	Gamma 90
Atom	X	Y	Z	Atom	X	Y	Z
Fe3	0.9923	0.2712	0.2596	Fe4	0.4923	0.2287	0.7403
Si1	0.4397	0.0943	0.2501	Si2	0.9397	0.4056	0.7498
O1	0.2233	0.8953	0.7627	O2	0.2766	0.3953	0.7627
O3	0.3252	0.9429	0.2381	O4	0.1747	0.4429	0.2381
O5	0.2721	0.1696	0.0276	O6	0.2984	0.1791	0.4592
O7	0.7721	0.3303	0.9723	O8	0.2015	0.6791	0.4592

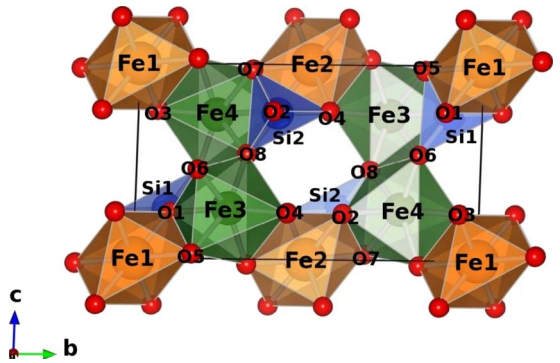

FIG. 3. (Color online) Optimized structure of configuration 1. The various categories of inequivalent atoms have been marked.

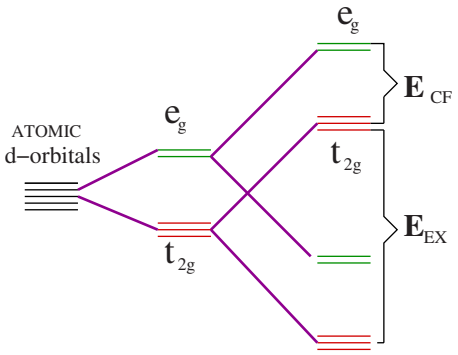

FIG. 4. (Color online) Schematic of the energy level splitting of the *d* orbitals at the Fe site.

M1 sites and that of Fe^{3+}-like ions into M2 sites give rise to a charge ordered pattern as shown in Fig. 6. The charge density has been calculated in a narrow energy window close to the Fermi level. Within this energy range, there is negligible contribution from Fe at M2 (which is close to the 3+ state), whereas for Fe at M1 (which is close to the 2+ state) there is a sharp peak in the down-spin channel of the *d* orbital. This peaking as already stated, is due to the presence of a single electron in the down-spin channel for Fe1 and Fe2 in high spin d^6 configuration. The charge density calculated in this energy interval therefore shows the accumulation of charge around M1 site whereas the M2 site remains devoid of any charge. This distribution of cations and vacancies is supported by experimental studies such as atomic resolution transmission electron microscopy,[17] which is driven by the structural distortion that happens due to introduction of vacancy. In our earlier communication we have shown that for a mixed Fe-Mg olivine system, Fe^{2+} prefers to occupy the smaller sized M1 sites, which is driven by the delicate balance between size consideration and covalency effect. While the Fe-O covalency is similar between Fe^{2+} and Fe^{3+}, their ionic sizes are rather different: Fe^{2+} cation (0.76 Å) is larger than Fe^{3+} cation (0.65 Å). The introduction of vacancies on the other hand reduces the volume of $M2O_6$ octahedra substantially, making them smaller compared to $M1O_6$ octahedra. It is therefore mere size consideration that dictates the preference of M2 sites by Fe^{3+}-like ions and M1 sites by Fe^{2+}-like ions.

2. Magnetic ordering

Finally, we turn on to magnetic ordering of Fe ions. The magnetic interaction between partially filled Fe ions mediated by oxygen ions are expected to be superexchange driven antiferromagnetic interaction. In case of fayalite the antiferromagnetic order has been confirmed both experimentally and theoretically.[6,32] There are however two antiferromagnetic configurations that are possible, as shown in Fig. 7. In one case (configuration A) the Fe spins within the zigzag chain consisting of neighboring M1-M2 sites are antiferromagnetically aligned while the interchain interaction is ferromagnetic. In the second case (configuration B), the intrachain interaction is ferromagnetic while the interchain interaction is antiferromagnetic. The total energies corresponding to both magnetic configuration A and B are listed in Table VI corresponding to different vacancy configurations. In all case, the magnetic configuration B, which satisfies AFM interchain interaction and FM intrachain interaction are found to be stable. The same magnetic arrangement was obtained also for pure fayalite compound.[6] Note this leads to strong antiferromagnetic Fe^{3+}-O-Fe^{3+} superexchange between corner-shared, two inter chain $M2O_6$ octahedra as well as strong antiferromagnetic Fe^{2+}-O-Fe^{3+} superexchange between corner-shared, interchain $M1O_6$ and $M2O_6$ octahedra while the edge-shared interactions between $M1O_6$ and $M2O_6$ octahedra within a given chain remains ferromagnetic. Though the strong antiferromagnetic nature of interchain Fe^{3+}-O-Fe^{3+} superexchange is in agreement with the predictions of Kan and Coey,[18] our DFT-predicted magnetic configuration is different from that speculated by Kan and Coey,[18] which would lead to magnetic configuration with no specific spin arrangement within a given chain. We found that the magnetic structure proposed by Kan and Coey[18] to be about 160 meV higher in energy than that given by the DFT-predicted ground-state magnetic structure (configuration B).

TABLE V. Structural comparison between fayalite, laihunite, and vacancy-bearing fayalite in configuration 1 (double vacancies at M1 sites).

	Fayalite (Fe_2SiO_4)	Laihunite	Configuration1
M1-O (av. Bond length) (Å)	2.15	2.19	2.11
volume of octahedra (Å^3)	13.25	14.01	12.53
M1-O(RMS deviation)	0.05	0.07	0.06
M2-O (av. Bond length) (Å)	2.18	2.04	2.02
volume of octahedra (Å^3)	13.81	11.32	10.99
M2-O(R.M.S deviation)	0.10	0.09	0.08

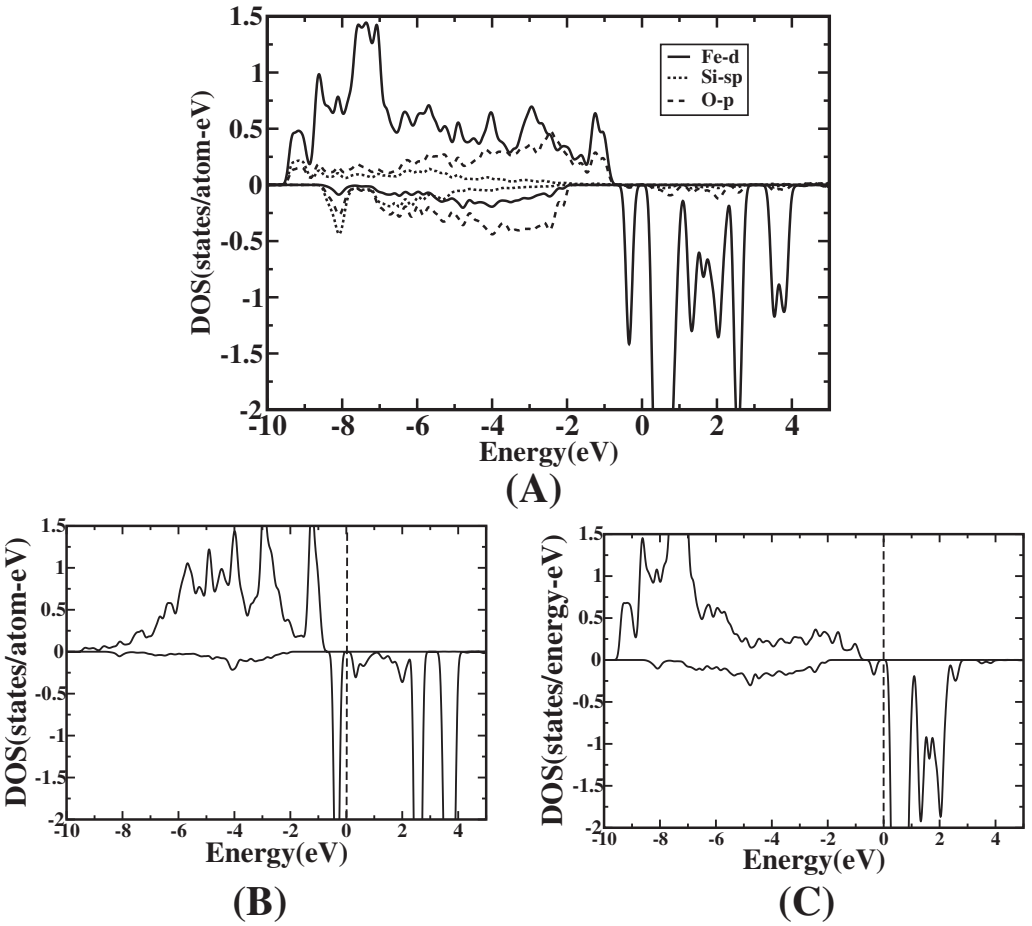

FIG. 5. (A) Partial density of states for configuration1 as shown in Fig. 2 projected onto Fe *d*, O *p*, and Si *sp* states; (B) partial DOS showing the Fe *d* orbital for Fe at M1 site; (C) partial DOS of Fe *d* orbital for Fe at M2 site. Within each panel the upper (lower) subpanel corresponds to majority (minority) spin. The negative of DOS has been plotted for the minority spin channel. The zero of the energy is set at the LSDA+*U* calculated Fermi energy [drawn as vertical dashed lines in (B) and (C)].

IV. CONCLUSION

We have carried out first-principles calculation of fayalite compound upon introduction of vacancy. Our study consists of structural optimization, study of electronic and magnetic structure. Our first-principles optimized geometry with two vacancies introduced at preferred M1 cationic sites in a unit cell of 4 f.u. leading to a chemical composition of $\square_{0.5}Fe_{1.5}SiO_4$ show good agreement with the structural details of naturally forming, vacancy-bearing compound, laihunite of formula $\square_{0.4}Fe_{1.6}SiO_4$. This provides reliability of DFT calculations in description of complex minerals with defect structure. The study of electronic structure shows that the introduction of vacancy leads to charge disproportionation at Fe site with Fe^{2+}-like ions occupying octahedra of site symmetry M1 of the fayalite lattice and Fe^{3+}-like ions occupying octahedra of site symmetry M2 of the fayalite lattice. This is caused by the specific site preference of the vacancy formation and the accompanying structural relaxation, which reverts the size relationship between $M1O_6$ and $M2O_6$ octahedra of the original fayalite lattice. The

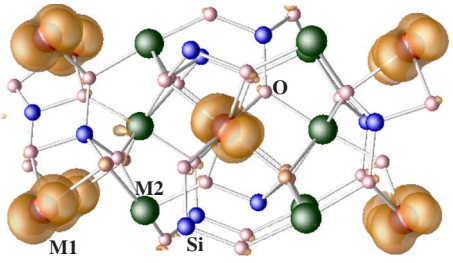

FIG. 6. (Color online) Charge-density plot for fayalite with double vacancies at M1 sites as in configuration 1. Contour height is set at 0.004/Å^3.

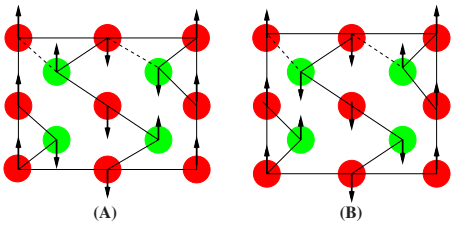

FIG. 7. (Color online) The two possible antiferromagnetic order in fayalite. Solid lines show the intrachain and dashed lines show the interchain interactions. Red (dark) and green (light) filled circles represent M1 and M2 sites.

TABLE VI. Total energy of the three structures with double vacancies at M1 sites in the two types of possible antiferromagnetic configuration as shown in Fig. 3.

	AF order	
Configuration	Configuration A energy (eV)	Configuration B energy (eV)
Configuration 1	−208.57	−208.70
Configuration 2	−208.48	−208.62
Configuration 3	−206.92	−207.02

preferential occupancy of Fe^{2+}-like and Fe^{3+}-like ions in M1 and M2 sites leads to charge ordering within the zigzag chain of M1-M2 at $T=0$ K which are found to be antiferromagnetically ordered. Finally, our first-principles prediction of charge ordered state in laihunite lists this compound in the category of interesting compounds such as manganites and magnetites, which should be experimentally verified. This may lead to study of charge order-disorder transition as a function of temperature, possible melting of charge-ordered phase by electric field to name a few. From the point of view of geological interest, our study will form the basis of study of vacancy diffusion in Fe bearing olivines, known as the transition-metal extrinsic diffusion.[9] This kind of diffusion is determined by both chemical potential and temperature as opposed to pure intrinsic or extrinsic diffusion and therefore depends on the ratio of Fe^{2+} and Fe^{3+} which would change dynamically as the vacancy propagates.

ACKNOWLEDGMENT

We acknowledge funding through Advanced Materials Research Unit.

*tanusri@bose.res.in

[1] M. H. F. Sluiter, V. Vinograd, and Y. Kawazoe, Phys. Rev. B **70**, 184120 (2004).
[2] R. M. Wentzcovitch, B. B. Karki, M. Cococcioni, and S. de Gironcoli, Phys. Rev. Lett. **92**, 018501 (2004).
[3] B. B. Karki, R. M. Wentzcovitch, S. de Gironcoli, and S. Baroni, Phys. Rev. B **62**, 14750 (2000).
[4] B. B. Karki, M. C. Warren, L. Stixrude, G. J. Ackland, and J. Crain, Phys. Rev. B **55**, 3465 (1997).
[5] R. M. Wentzcovitch, J. L. Martins, and G. D. Price, Phys. Rev. Lett. **70**, 3947 (1993).
[6] M. Cococcioni, A. Dal Corso, and S. de Gironcoli, Phys. Rev. B **67**, 094106 (2003).
[7] J. R. Smyth, Am. Mineral. **60**, 1092 (1975).
[8] S. A. T. Redfern, C. M. B. Henderson, K. S. Knight, and B. J. Wood, Eur. J. Mineral. **9**, 287 (1997).
[9] S. Chakraborty, J. Geophys. Res., [Solid Earth] **102**, 12317 (1997).
[10] M. Müller-Sommer, R. Hock, and A. Kirfel, Phys. Chem. Miner. **24**, 17 (1997).
[11] J. Chen, R. Li, J. B. Parise, and D. J. Weidner, Am. Mineral. **81**, 1519 (1996).
[12] S. Chatterjee, S. Sengupta, T. Saha-Dasgupta, K. Chatterjee, and N. Mandal, Phys. Rev. B **79**, 115103 (2009).
[13] O. Tamada, B. Shen, and N. Morimoto, Mineral. J. **11**, 382 (1983).
[14] M. W. Schaefer, Nature (London) **303**, 325 (1983).
[15] S. Matsuura, S. Sueno, and N. Yurimoto, Mineralogical Society of Japan, 1983 Annual Meeting Abstracts with Program, D29, p. 118.
[16] M. Kitamura, B. Shen, S. Banno, and N. Morimoto, Am. Mineral. **69**, 154 (1984).
[17] D. E. Janney and J. F. Banfield, Am. Mineral. **83**, 799 (1998).
[18] X. Kan and J. M. D. Coey, Am. Mineral. **70**, 576 (1985).
[19] P. Fu, Y. Kong, and L. Zhang, Geochemistry **1**, 115 (1982).
[20] I. Shinno, Phys. Chem. Miner. **7**, 91 (1981).
[21] E. J. W. Verwey, Nature (London) **144**, 327 (1939); E. J. W. Verwey, P. W. Haayman, and F. C. Romeijan, J. Chem. Phys. **15**, 181 (1947).
[22] S.-W. Cheong and H. Hwang, in *Colossal Magnetoresistive Oxides*, Monographs in Condensed Matter Science, edited by Y. Tokura, Chap. 7 (Gordon and Breach, Reading, UK, 2000).
[23] P. Hohenberg and W. Kohn, Phys. Rev. **136**, B864 (1964); W. Kohn and L. J. Sham, *ibid.* **140**, A1133 (1965).
[24] G. Kresse and J. Hafner, Phys. Rev. B **47**, 558 (1993); G. Kresse and J. Furthmüller, Comput. Mater. Sci. **6**, 15 (1996); Phys. Rev. B **54**, 11169 (1996).
[25] O. K. Andersen and O. Jepsen, Phys. Rev. Lett. **53**, 2571 (1984).
[26] P. E. Blöchl, Phys. Rev. B **50**, 17953 (1994); G. Kresse and D. Joubert, *ibid.* **59**, 1758 (1999).
[27] J. Hubbard, Proc. R. Soc. London **276**, 238 (1963).
[28] V. I. Anisimov, I. V. Solovyev, M. A. Korotin, M. T. Czyzyk, and G. A. Sawatzky, Phys. Rev. B **48**, 16929 (1993).
[29] W. E. Pickett, S. C. Erwin, and E. C. Ethridge, Phys. Rev. B **58**, 1201 (1998); V. I. Anisimov, I. S. Elfimov, N. Hamada, and K. Terakura, *ibid.* **54**, 4387 (1996).
[30] N. C. Richmond and J. P. Brodholt, Am. Mineral. **85**, 1155 (2000).
[31] Since the octahedra are in general distorted, there are further splittings within individual t_{2g} and e_g blocks. They are, however, much smaller compared to t_{2g}-e_g splitting.
[32] R. Müller, H. Fuess and P. J. Brown, J. Phys. Colloq. **C7**, C7 (1982).